

**ENVIRONMENTAL APPLICATIONS OF  
HIGH RESOLUTION TEM METHODS**

**Cris Mauldin-Mayerle, Norman R. Carlson, Kenneth L. Zonge**  
Zonge Engineering & Research Organization, Inc.  
3322 E. Fort Lowell, Tucson, Arizona, USA 85716

presented at

**The 4th Meeting on  
Environmental and Engineering Geophysics  
Barcelona, Spain September 14-17, 1998**

**European Section, EEGS**

## ENVIRONMENTAL APPLICATIONS OF HIGH RESOLUTION TEM METHODS

Cris Mauldin-Mayerle, Norman R. Carlson, Kenneth L. Zonge  
Zonge Engineering & Research Organization, Inc.  
3322 E. Fort Lowell, Tucson, Arizona, USA 85716

### INTRODUCTION

Though commonly used in minerals exploration, transient electromagnetic (TEM) methods are less common in environmental and engineering applications. Several aspects of the technique make it a very useful tool, including the flexibility of loop sizes and geometries, and the recent improvement in electronics that allow faster transmitter turn-off times, and therefore shallower soundings. Faster electronics also allow the acquisition of all three magnetic field components simultaneously, increasing the amount of information available for interpretation and modeling. Our discussion includes environmental applications of TEM data in standard geometries (such as in-loop, fixed-loop, etc.) but with higher resolution than usually obtained. In this case, "high resolution" refers to higher resolution spatially (much higher data density than is normally used in minerals exploration TEM) and temporally (much faster turn-off times and faster sample rates). Also of interest is the added benefit of utilizing the late time TEM data, after the background earth response has decayed, as a deep-sounding metal detection tool.

### LOOP GEOMETRIES

The differing sensitivities of various loop geometries and loop sizes is one of the most useful aspects of TEM methods, and the ability to change these parameters in the field is important. NanoTEM data acquired at the Idaho National Engineering Laboratory's (INEL) Cold Test Pit provide an excellent example of these different sensitivities. (Note: NanoTEM is the name of our fast turn-off TEM system.) The Cold Test Pit is a waste dump created specifically for studying waste dumps, and the pit characteristics and contents are well documented. In one part of the pit, there is a massive amount of metal in the

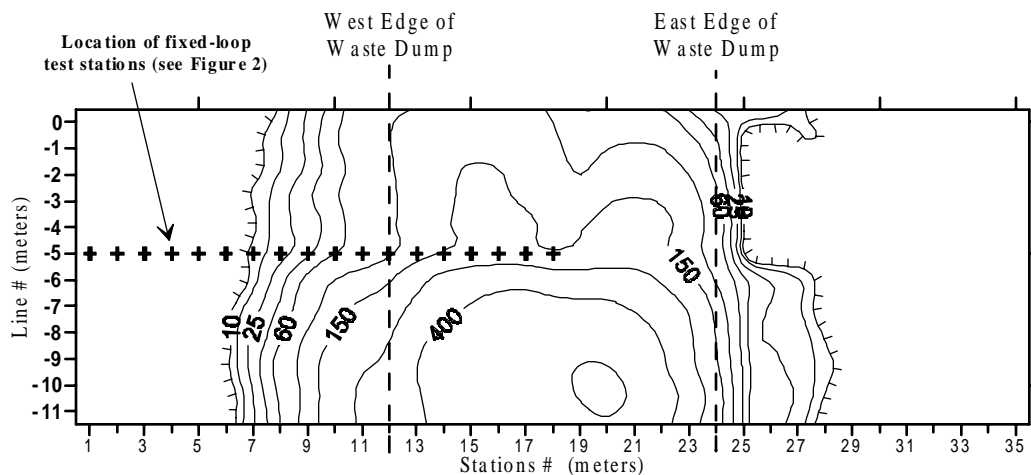


Figure 1: Plan view of in-loop TEM (Hz component) data for time window 12 (32.6 microseconds). This loop configuration results in a large anomaly associated with the waste dump, but does not delineate the edges very well.

Figure 2a

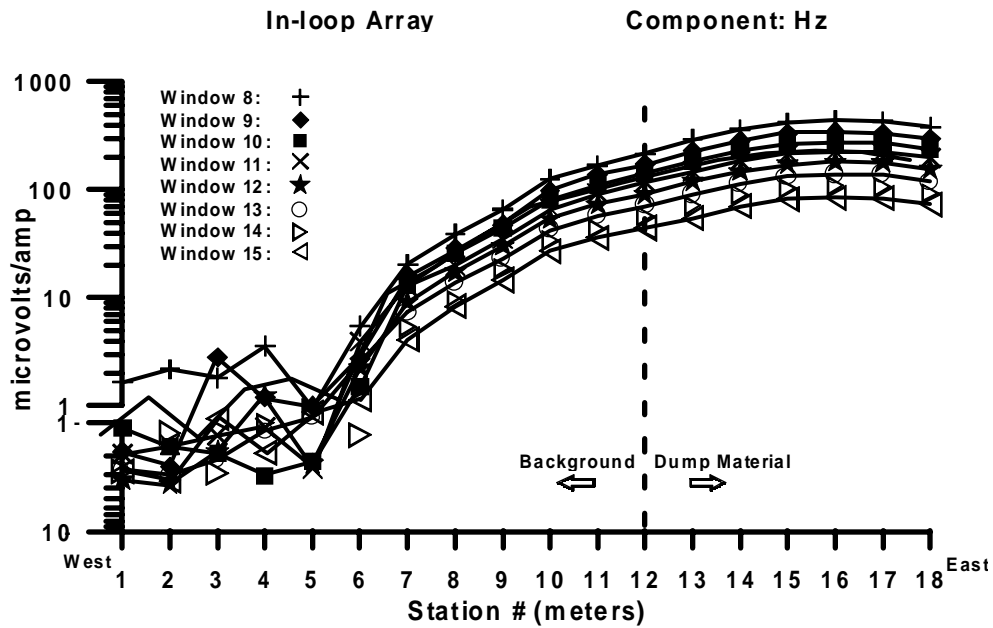
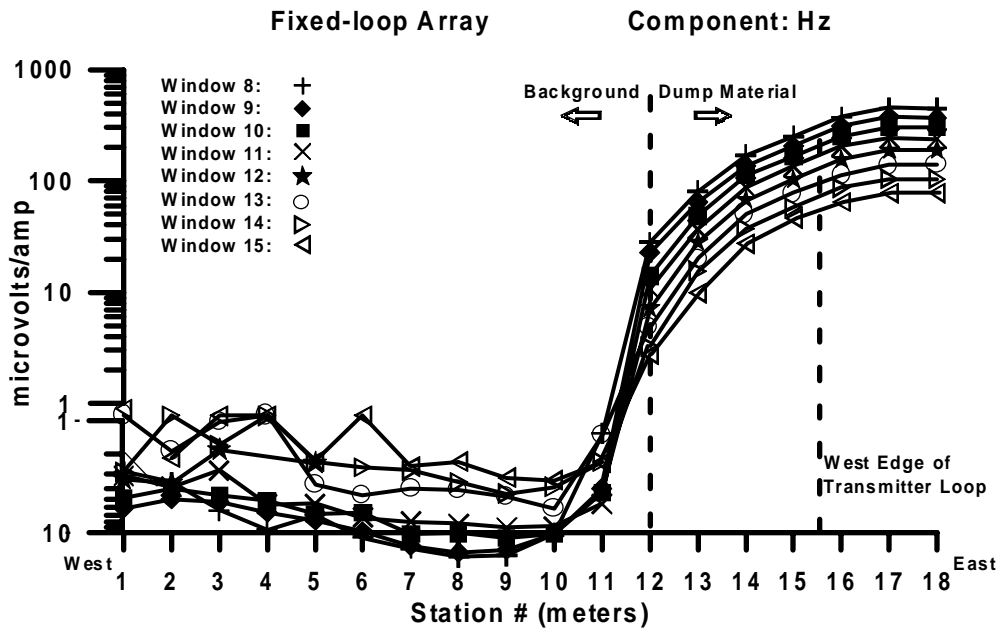


Figure 2b



form of barrels (some stacked as many as five barrels high) and boxes containing miscellaneous metals, buried under 1.5 to 2.5 meters of soil cap.

Data were acquired in this area in the in-loop configuration on a grid with lines and stations spaced at one meter intervals, and then, using the same equipment, a line of fixed-loop data was also acquired. For the in-loop survey, a 10 meter by 10 meter square transmitter loop was used, with a 1 meter by 1 meter square receiver loop. Thirty-six receiver loops were measured inside each transmitter loop in a 6 meter by 6 meter grid. Figure 1 shows a plan view of the late time results (Hz component) of the in-loop survey, comprised of 420 stations. Values are in microvolts/ampere, contoured logarithmically. Since the waste dump is large (relative to the transmitter loops) and massively metallic, the in-loop data show a very strong anomaly, but without well-defined edges.

For comparison, a line of fixed-loop data was also acquired, with a 5-meter square transmitter loop placed on the dump while reading 1-meter square receiver loops moving away from the transmitter. Figure 2 shows the Hz component data from both the in-loop (Figure 2a) and fixed-loop (Figure 2b) arrays in profile form, for eight of the late time windows, which is after the background earth response has decayed. In the fixed-loop configuration, the edge of the dump is very clearly delineated, while the in-loop configuration shows no indication of the location of the dump edge. Thus, in projects where edge delineation of strong conductors is important, the fixed loop array may be preferable.

In contrast, when the target or targets are small relative to the transmitter loop, in-loop TEM data are extremely useful, particularly when used as a deep metal detector. If the loop sizes and transmitted currents are properly configured, the data acquired after the background earth response has decayed to near-zero are very useful. For example, Figure 3 shows the measurements at three stations (two readings are shown for each station); one station is directly over a buried well casing, one station is one meter east of the casing and the other station is one meter south of the casing. In the first 10 time windows, the data are very repeatable and similar for all three stations. These first 10 windows can be used for modeling the shallow geology. After 500 microseconds, however, the stations that are not directly over the casing have decayed into random, near-zero noise; note that the magnitudes are very small and the repeatability of the data is very poor. Directly over the casing at station 4621, however, the data are still repeatable and elevated above random background noise. Thus the early time windows can be used to map shallow geology, and the later time windows of the same data set can be used as a deep metal detector.

Figure 4 shows a more extensive example of the use of TEM as a deep metal detector. These data were acquired on the north end of the I.N.E.L. Cold Test Pit, in an area called the Calibration Cell. In this area, discrete objects such as individual barrels, filing cabinets, and boxes are buried under approximately 2.5 meters of soil. For this survey, 10 meter by 10 meter square transmitter loops were again used, with 1 meter by 1 meter square receiver loops. This figure shows the average of windows 21 through 26, after the background earth response has decayed, thus enhancing features with very long time constants. Anomalous peaks are associated with most targets, although the dense-pack metals and filing cabinets combine to create one large anomalous area. Two of the targets created no anomalies; one is the box containing wood and paper, and the other is a 30 gallon plastic drum containing saltwater. The wood/paper target was not expected to show an anomaly, but it is not clear why the saltwater target is not anomalous. Since the targets had been buried for at least four years prior to this survey, it is possible that the saltwater had leaked out of the plastic drum.

**Figure 3**

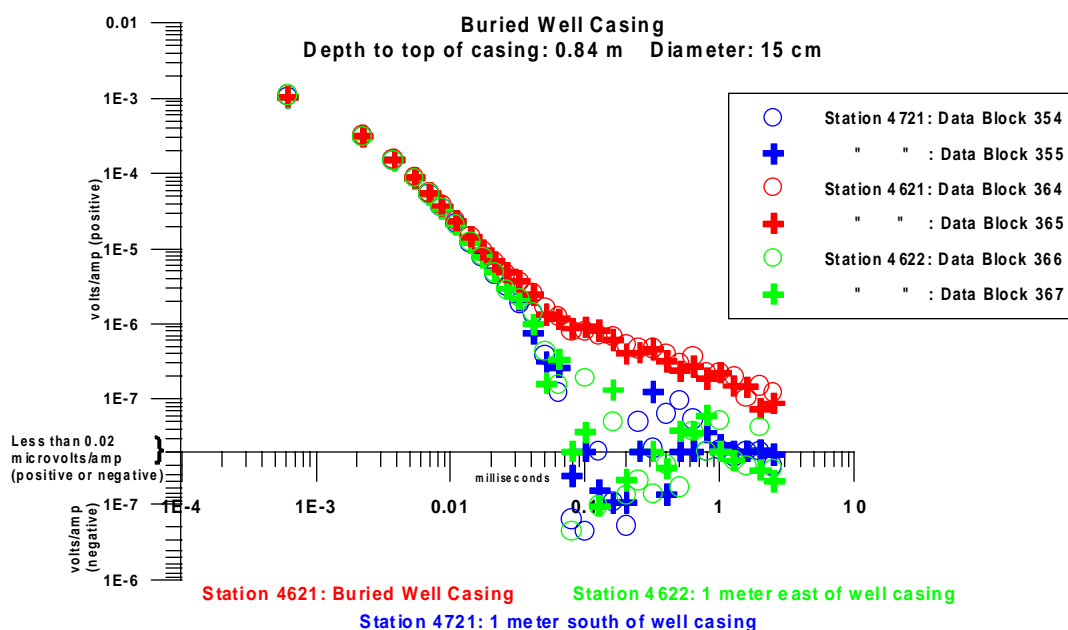


**Figure 4**

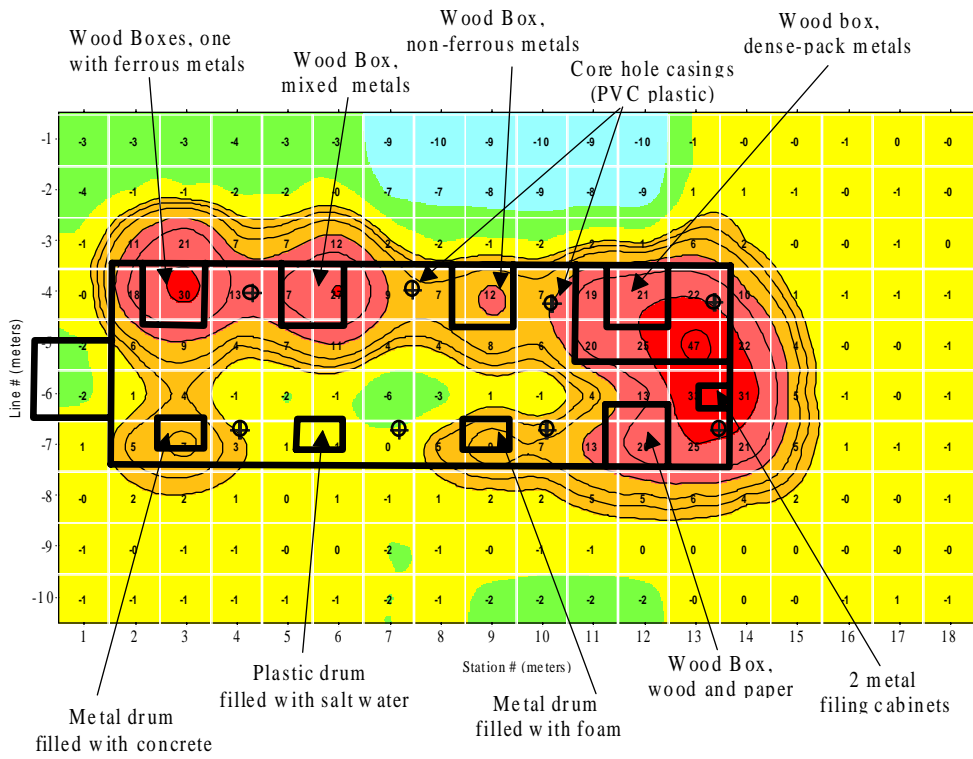
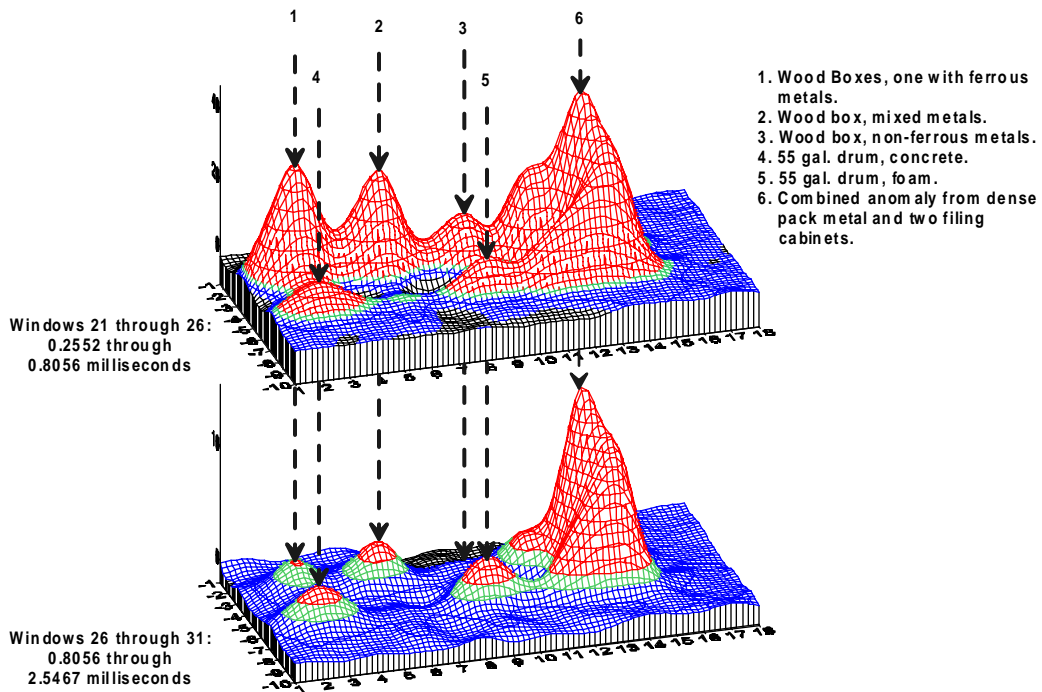


Figure 4: Plan view of in-loop TEM data (Hz component) for several late time windows over the INEL Calibration Cell. Values shown are the average of windows 21 through 26 in microvolts/am pere, c ontoured logarithmically.

**Figure 5**



Windows 21 through 26:  
0.2552 through  
0.8056 milliseconds

Windows 26 through 31:  
0.8056 through  
2.5467 milliseconds

1. Wood Boxes, one with ferrous metals.
2. Wood box, mixed metals.
3. Wood box, non-ferrous metals.
4. 55 gal. drum, concrete.
5. 55 gal. drum, foam.
6. Combined anomaly from dense pack metal and two filing cabinets.

Figure 6

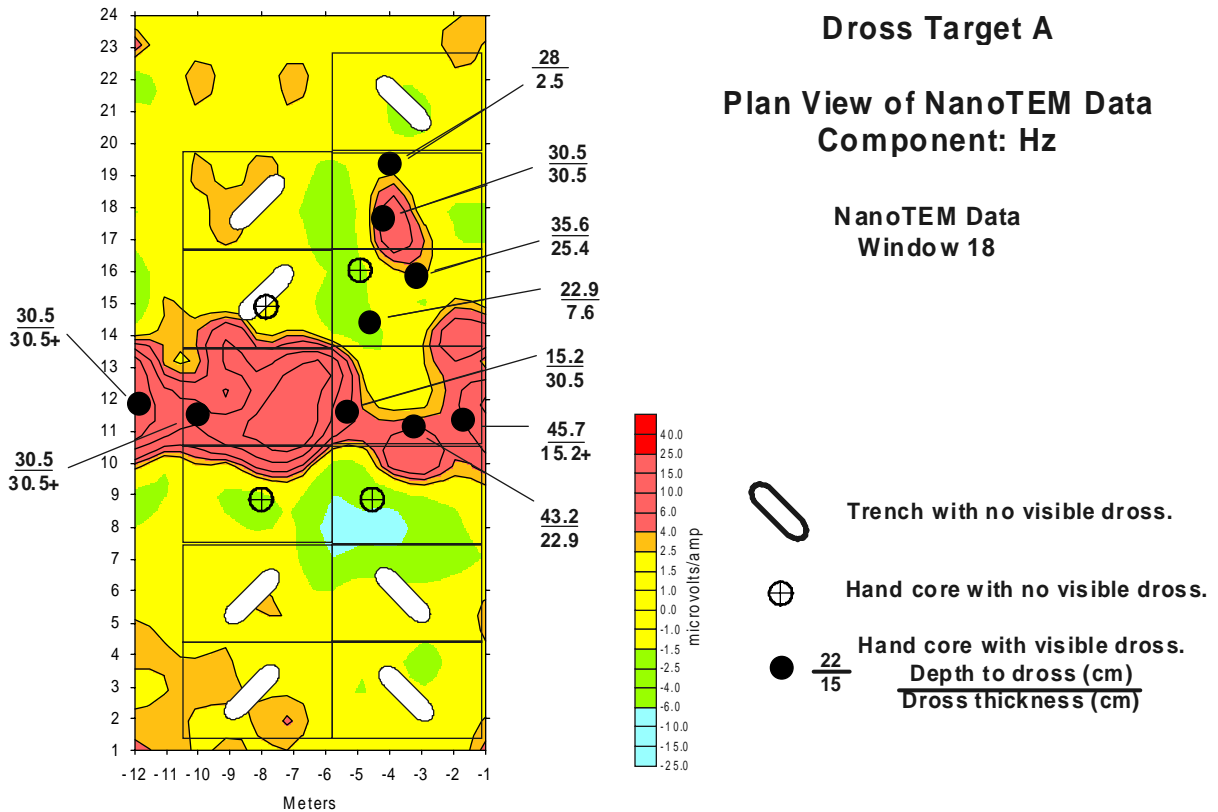


Figure 5 shows the same data in addition to the data from six later time windows. These data are plotted with the z-axis as magnitude, in order to show graphically how the anomalies change with time. The bottom plot has been scaled (in the z-axis) such that the anomaly labeled “6” is the same size in both plots. In this way, it is possible to see that the different anomalies are changing in time at different rates. Notice, for example, that in the upper plot, the anomalies associated with the metal in wooden boxes (1, 2, and 3) are all stronger than anomalies associated with the metal drums (4 and 5). In the lower plot, however, the metal drums are unchanged, indicating that the anomalies are decaying at approximately the same rate as anomaly 6. Anomalies 1, 2, and 3 are now smaller than features 4 and 5, suggesting that the decay time constant is different for the different objects. Our research is continuing into whether a careful analysis of decay time constants can be used in some situations to better discriminate targets.

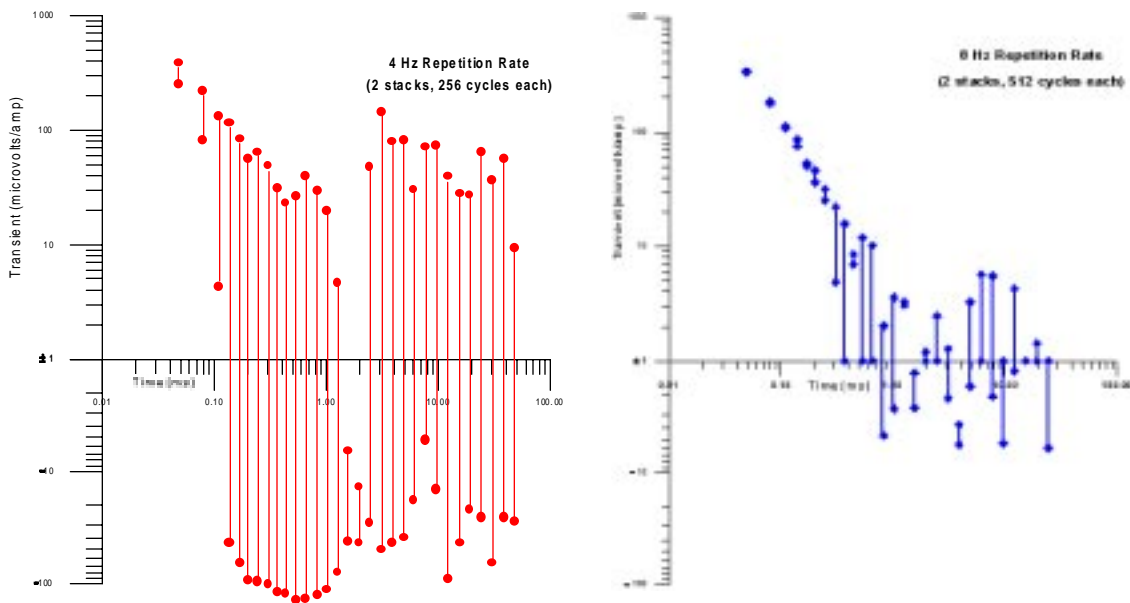
The target need not be discrete, metallic objects, of course. On one recent project, the target was aluminum dross, which had been dumped at various locations in the desert near Tucson several decades ago by aircraft recycling companies. The dross is in the form of a grayish-silver powder, though it sometimes contains solid conglomerations that have the appearance of being cemented or silicified, and it is usually buried under a few meters of soil. The dross contains lead and cadmium, and is therefore a health hazard. Since this desert area has now been developed, containing houses, a school, and a public park, it became important to locate and remediate the dross. Figure 6 shows the contoured NanoTEM data over one of the target areas, along with information from subsequent trenching and core holes. This data set was also acquired using a 10 meter square transmitter loop and 1 meter square receiver loops. The TEM data are in excellent agreement with the physical sampling; the strongest anomalies are associated with the thickest sections of dross, and areas free of anomalies show no evidence of dross.

**Figure 7**

Repetition Rate	50 Hz Power		60 Hz Power	
	5.0 MHz Crystal	4.980736 MHz Crystal	5.0 MHz Crystal	4.980736 MHz Crystal
1 Hz	250 : 1	10000 : 1	333 : 1	10000 : 1
2 Hz	80 : 1	NONE	700 : 1	10000 : 1
4 Hz	250 : 1	10000 : 1	50 : 1	NONE
8 Hz	250 : 1	10000 : 1	20 : 1	10000 : 1
16 Hz	140 : 1	10000 : 1	700 : 1	10000 : 1
32 Hz	2000 : 1	10000 : 1	2000 : 1	10000 : 1

Figure 7: Noise rejection of powerline noise for various repetition rates in TEM using two different timing crystals.

**Figure 8**



### CULTURAL NOISE CONSIDERATIONS

Technological advancements have provided an improved ability to work in the presence of active powerline noise. For example, in recent years, timing crystals have become available that provide better noise rejection due to small changes in the crystal frequency. Figure 7 shows a comparison between the noise rejection using an older 5.0 MHz crystal and a more recently available 4.980736 MHz crystal. The difference in noise rejection arises from the small difference in the actual repetition rate of the data acquisition relative to the 50 Hz or 60 Hz noise. For example, using a 5.0 MHz crystal, the 4 Hz repetition rate is actually occurring at 4.015 Hz, whereas using the 4.980736 MHz crystal, the 4 Hz repetition rate occurs exactly at 4.0 Hz. As waveforms are stacked and averaged, this small difference becomes very important, as is evident from Figure 7.

In actual field environments, of course, cultural noise is not usually as simple and stable as in the laboratory. Powerline noise is not always exactly 50 Hz or 60 Hz, there are higher odd harmonics which can be a problem, and there are other noisy frequencies (120 Hz from pipeline cathodic protection, for example). Despite all of these complicating factors, the differences in noise rejection are evident in the field. For example, note that with the 4.980736 MHz crystals in the presence of 60 Hz powerline noise, the noise rejection at most repetition rates is 10,000:1, but at a repetition rate of 4 Hz, there is no noise rejection. As a result, in the USA, our crews never acquire TEM data at a 4 Hz repetition rate. A recent survey at a buried landfill provides a good example of this characteristic. Figure 8 shows two sets of data taken at the same location using the same equipment in the vicinity of large powerlines. In both cases, the transmitted current was 7 amps into a 40 meter by 40 meter square loop. On each plot, two readings are shown; one plot shows the readings acquired at 4 Hz and the other shows the data acquired at 8 Hz. The number of cycles that were stacked and averaged were deliberately short, but it is clear that even with short stacks, the first seven windows of the 8 Hz data are repeatable and useful. Longer stacks (more cycles) or higher transmitted currents would probably provide even deeper data. The data at 4 Hz, however, are very noisy. Note that even in the late times, when amplitudes should be decaying to zero, we have high amplitude (both positive and negative), unrealistic data.

### MULTI-COMPONENT ADVANTAGES

Perhaps the most significant technological improvement in recent years is the ability to acquire all three components of TEM data simultaneously at very fast sample rates. In the past, the most common TEM data set consisted of the Hz (vertical) component only, because it was the most straightforward data set to interpret. There is also considerable information in the Hx and Hy components, but interpretation was considered more difficult. Although 3-D, 3-component inversion modeling is still not yet readily available, the Hx and Hy component data are very useful. One good example is from one of the grids from the I.N.E.L. Calibration Cell; within this transmitter grid are two discrete targets, one consisting of ferrous metals and one containing mixed metals. On Figures 9, 10, and 11, these targets are shown as black rectangles. The data values shown are in microvolts/amp, contoured and colored on a logarithmic scale. The data values are plotted in the center of each receiver loop. The data were acquired in the in-loop array, reading 36 one meter by one meter receiver loops inside the 10 meter by 10 meter transmitter loop.

Figure 9a shows the first window for all three components in plan view for the calibration cell grid and Figure 9b shows the data for a nearby grid where there are no known buried objects (called the background grid). As expected in the background grid, the Hx and Hy data are dipolar, going from strongly positive (shaded red) near the north or west transmitter wires (for Hx and Hy respectively) to strongly negative (shaded blue) near the south or east transmitter wires. Hz is positive throughout the grid. In a homogeneous earth, the Hx and Hy would be near zero in the center of the grid (center of the transmitter loop). The bias of the Hy data is discussed below.

In the grid that contains targets (the calibration cell grid), the window 1 Hx data are also dipolar but less uniform than the background grid. The Hy data are significantly different from background; dipolar effects can be seen associated with the two targets, and this grid is obviously very different from background. The Hz data are relatively uniform, with no strong indications of anomalies.

As time progresses, we see even stronger differences between the background data and the data over the targets. At 5 microseconds after turn-off (Figures 10a and 10b), the dipolar nature of Hx is still evident in the background data, but the Hy background data are uniformly positive. In a truly homogeneous background, we would expect the Hy data to be dipolar from west (positive) to east (negative). In this case, however, a massive conductor (the Cold Test Pit itself) is six meters east of the background grid. Even though there is no conductor within the background transmitter loop, the Hy data are apparently being influenced by the nearby Cold Test Pit. In some cases, this could be useful information; although the grid of data did not detect any anomalies, it is apparent that a strong anomaly lies to the east of the grid.

Over the targets, the dipolar anomalies in this window are clearly evident, and could be used to pinpoint the targets even without the Hz data. The anomalies are also becoming evident in Hz.

By window 8, at 14 microseconds (Figure 11a and 11b), the background grid has already decayed into random near-zero noise levels. The effects from the targets are still strong, however, continuing to show dipolar anomalies in Hx and Hy. Of

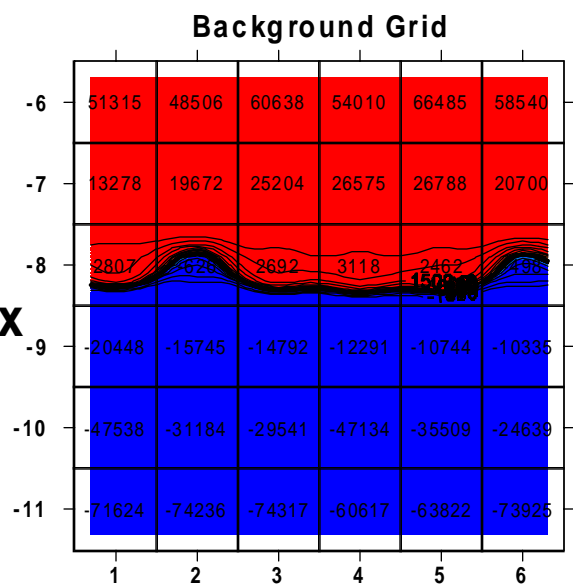
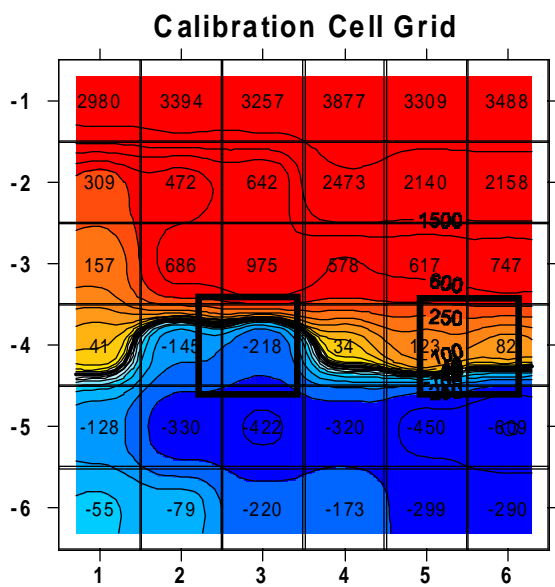


interest is the fact that the anomalies in Hx and Hy (adjacent to the targets) are stronger than the Hz anomalies at the same stations. Thus even though we have already seen that the Hz data provide very good lateral resolution for pinpointing the location of a target, the Hx and Hy data may be useful in detecting targets from a greater distance. Thus with on-board processing and smart search algorithms (such as neural networks), it may be possible in some cases to optimize data acquisition, using Hx and Hy to detect targets at a distance, and the combination of Hx, Hy, and Hz to pinpoint locations.

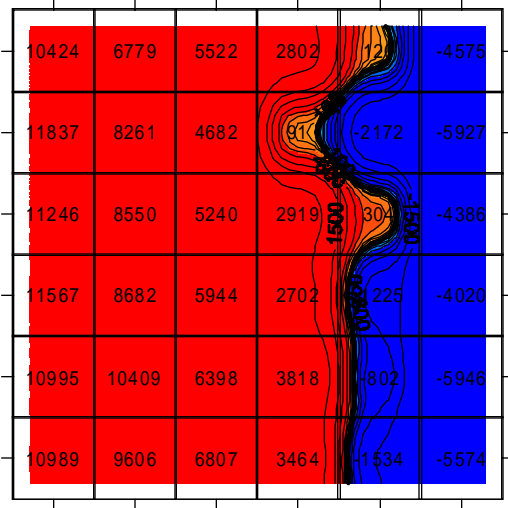
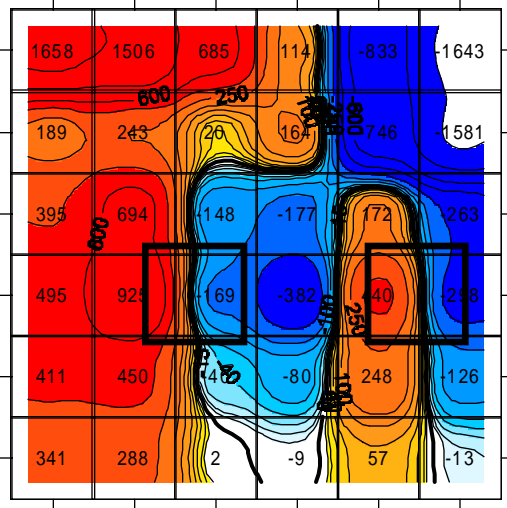
The anomalies associated with the two targets continue through the later time windows lasting over 500 microseconds after transmitter turn-off. Conversely, in the background grid, the background earth response had decayed to near-zero within 14 microseconds in this high resistivity environment. By the time we reach window 26 at 800 microseconds, there is no evidence of the targets in any of the components.

## **SUMMARY**

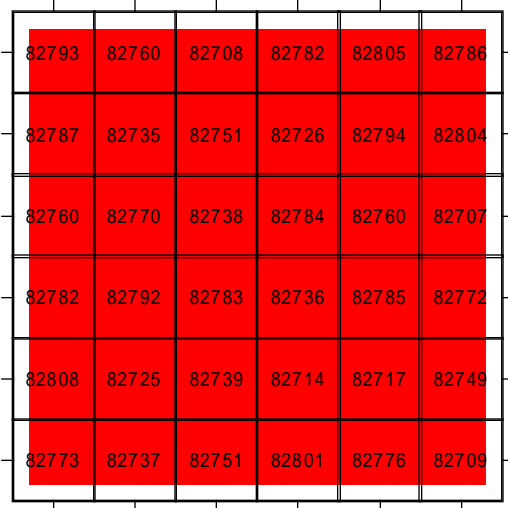
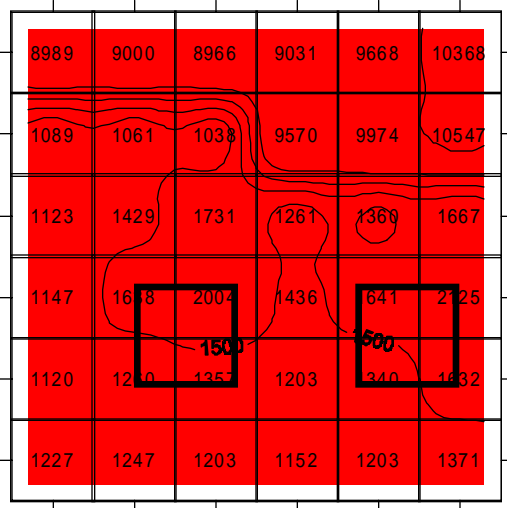
TEM methods can be extremely useful in high resolution environmental surveys, particularly when the equipment system allows rapid and easy changes in loop geometries to take advantage of the differing sensitivities of loop arrays. Small, discrete targets can be located with in-loop surveys, while boundaries of large targets are often better delineated with fixed-loop methods. Recording a large number of windows along the decay curve allows the system to be used as both a resistivity sounding tool as well as a deep metal detector, and the decay time constants may eventually prove useful in target characterization. Most significantly, by recording all three magnetic field components, substantial additional information is available to help optimize field surveys and improve interpretation of the data.



Hx



Hy



Hz

Figure 9a

Figure 9b

Window 1: 0.6 microseconds

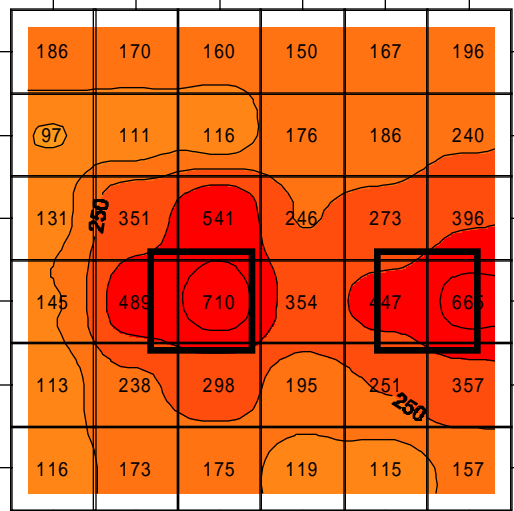
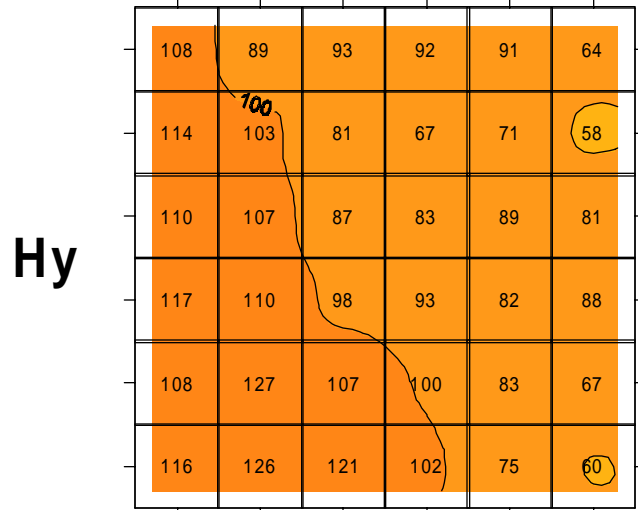
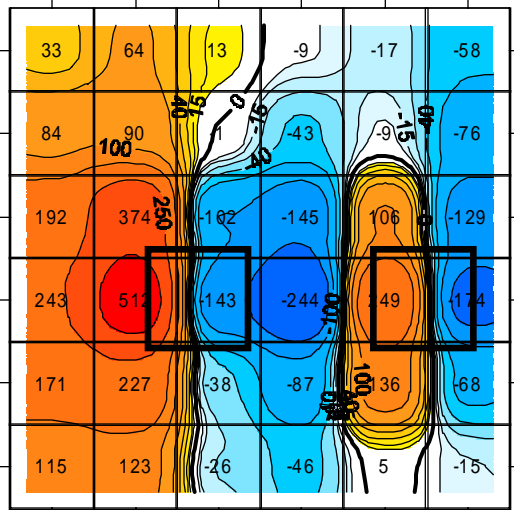
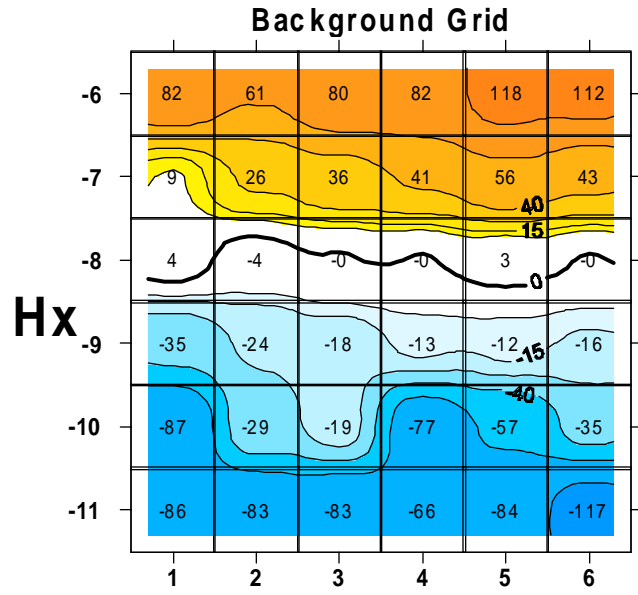
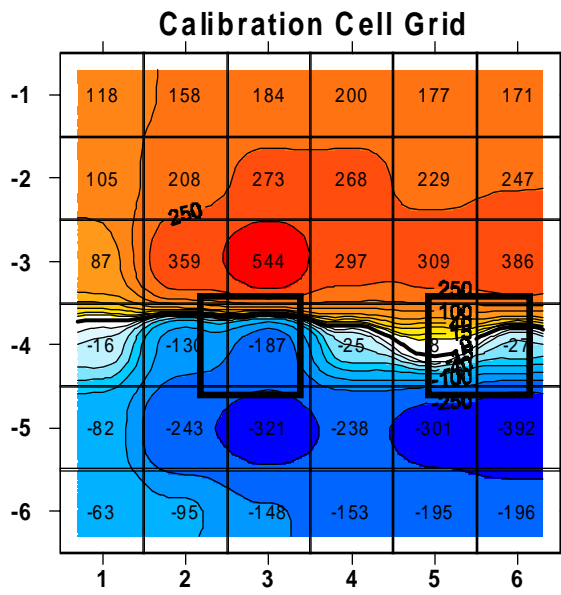


Figure 10a

Figure 10b

Window 4: 5.44 microseconds

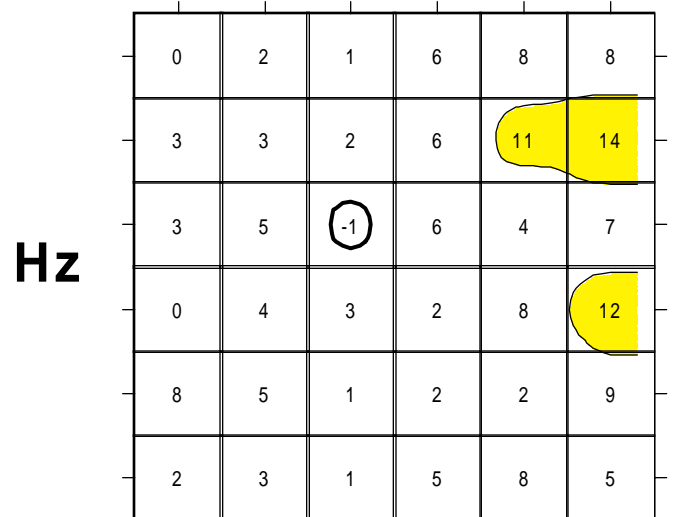
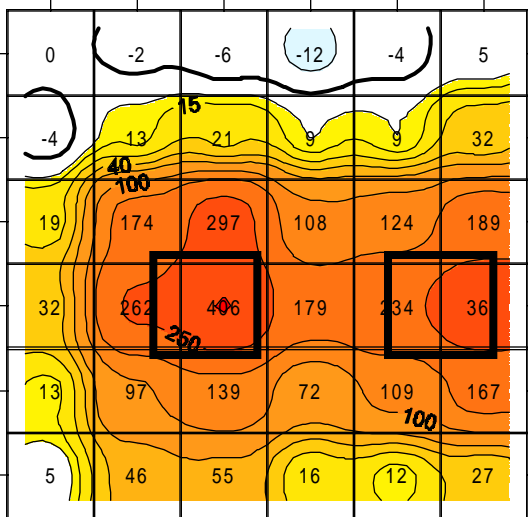
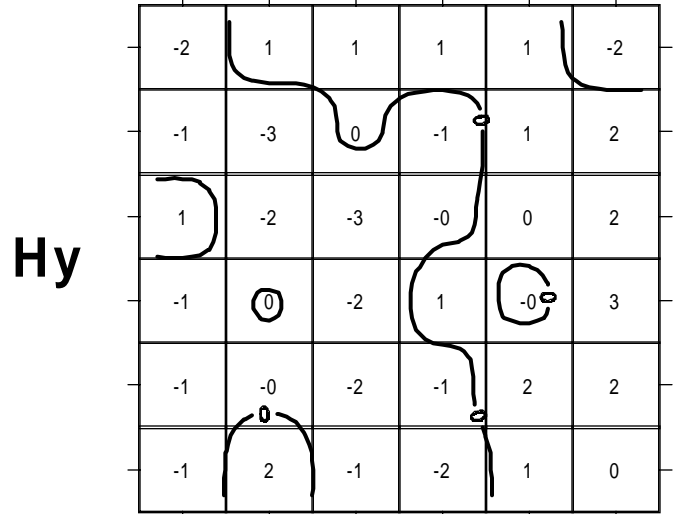
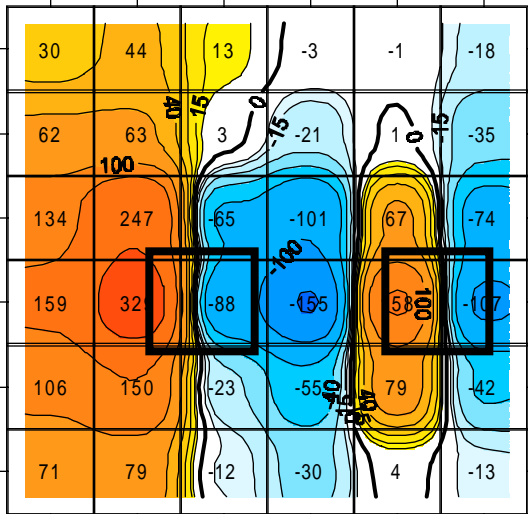
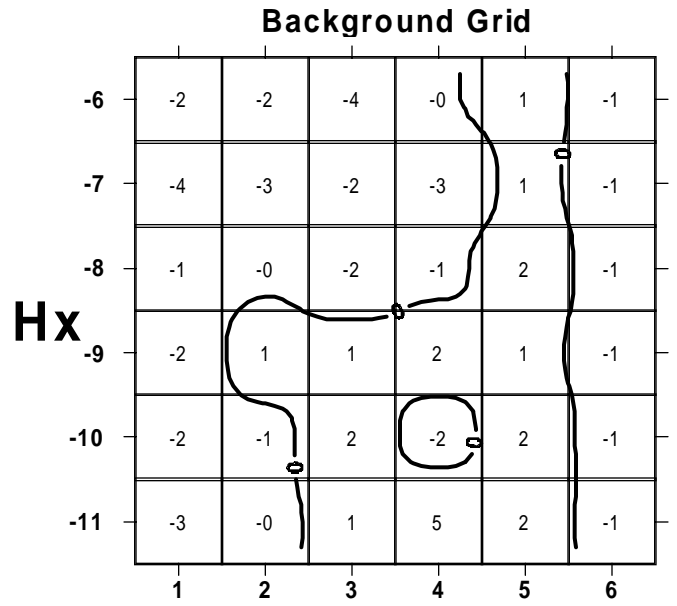
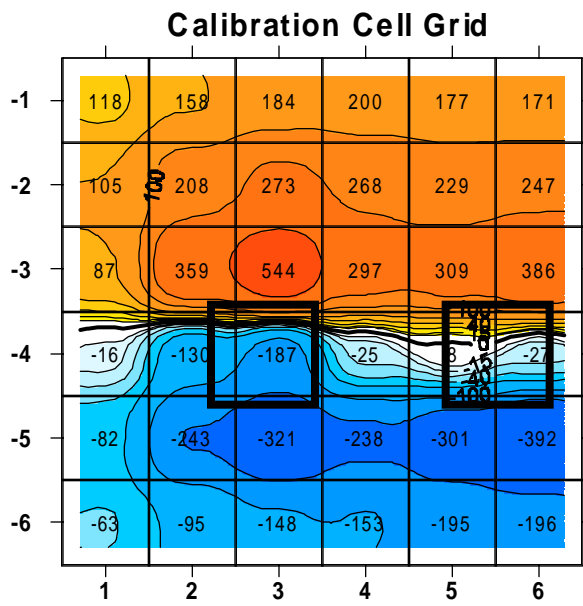


Figure 11a

Figure 11b

Window 8: 14.2 microseconds